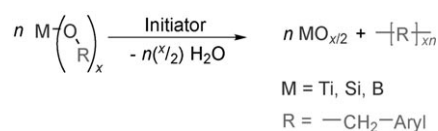


Nanoscale Tungsten Trioxide Synthesized by In Situ Twin Polymerization**

Falko Böttger-Hiller, Ralf Lungwitz, Andreas Seifert, Michael Hietschold, Maik Schlesinger, Michael Mehring, and Stefan Spange*

Nanoscale metal oxides and control of their structures is an intensively studied scientific field because of the manifold industrial applications of such materials.^[1] Most synthetic routes in homogenous solution require additives to control the morphology. Only a few synthetic methodologies do not need any templates. In such approaches, the reaction process intrinsically leads to nanostructured metal oxides. The non-aqueous sol-gel process (NASG)^[2] and twin polymerization (TP),^[3] which was developed in our group, are two such template-free syntheses. TP is defined as the simultaneous formation of two polymers in one process. To date, silicon, titanium, and boron monomers synthesized from several aryl methanol derivatives were transformed into metal oxide/polymer nanocomposites using TP (Scheme 1).^[3] In the



Scheme 1. Reaction scheme of twin polymerization.

formation of the composite material, the organic compound acts as a template for the inorganic component and vice-versa.

The oxidation of the organic polymer in air leads to a porous inorganic oxide, which is characterized by its nanostructure and its very high specific surface area (up to 700 m² g⁻¹).^[3]

The motivation and aim of this work was the synthesis of nanoscale tungsten oxide by TP to demonstrate the potential

and the limits of the method compared to the NASG process. In a recently published article about an NASG preparation of WO₃, inorganic precursors such as tungsten alkoxides reacted with benzyl alcohol directly to give tungsten oxide or tungsten hybrid materials with a molecular organic component.^[2a,4] There are two interesting aspects of the non-aqueous sol-gel process: the resulting oxides are halide-free, and the variation of the reaction parameters could be used to achieve extraordinary morphologies, such as nanorods.^[4]

On an industrial scale, tungsten oxide is usually prepared by annealing tungsten^[5] and by calcination^[6] of ammonium paratungstate. Because of its catalytic,^[7] photochromic,^[8] and electrochromic^[9] properties, tungsten oxide is used for anti-dazzle mirrors,^[10] “smart” windows,^[11] gas-sensing devices,^[12] and photocatalysts.^[7a] Some of these applications depend critically on the accessible surface area. For nanoscale tungsten trioxide, the published values for Brunauer–Emmet–Teller (BET) surface areas range from 10 to 26 m² g⁻¹.^[7,12]

To produce nanoscale tungsten trioxide with a higher BET surface area, we planned to synthesize a tungsten-containing monomer W(OR)₆ with a cationic polymerizable aryl methanol derivative, such as thiophene-2-methanol, *p*-methoxybenzyl alcohol (*p*-MBA), or *o*-methoxybenzyl alcohol (*o*-MBA; see the Supporting Information). However, the aryl methanol species did not react with WCl₆ to the target monomers; instead, tungsten oxide/polymer hybrid materials (HM) resulted in one step. Surprisingly, the morphology of these particles resembled the titanium dioxide, silicon dioxide, and boron oxide/polymer nanocomposites that were produced by TP of elaborate monomers. It must be stressed that nanostructured HMs only resulted if there was no base added to the mixture, which should bind the HCl that is formed. When organic bases such as *N*-methylimidazole and proton sponge (1,8-bis(dimethylamino)naphthalene) were used,^[13] compact hybrid materials without a nanostructure were obtained.

The organic components of the HMs are insoluble in moderately polar organic solvents such as dichloromethane. The HMs show very small specific surface areas (Table 1) and structural features in the micrometer range.

Energy-dispersive X-ray spectroscopy (EDS) measurements (see the Supporting Information) reveal homogeneously distributed elements in the completely amorphous HMs, as known from the SiO₂/polymer or TiO₂/polymer hybrid materials produced by TP.^[3] The TEM (transmission electron microscopy) images of the HMs show structural features on a scale of about 20 to 50 nm.

[*] F. Böttger-Hiller, R. Lungwitz, Dr. A. Seifert, Prof. Dr. S. Spange
Professur für Polymerchemie
Technische Universität Chemnitz
Strasse der Nationen 62, 09111 Chemnitz (Germany)
Fax: (+49) 371-5312-1239
E-mail: stefan.spange@chemie.tu-chemnitz.de

M. Schlesinger, Prof. Dr. M. Mehring
Professur für Koordinationschemie
Technische Universität Chemnitz
Strasse der Nationen 62, 09111 Chemnitz (Germany)
Prof. Dr. M. Hietschold
Professur Analytik an Festkörperoberflächen
Technische Universität Chemnitz
Strasse der Nationen 62, 09111 Chemnitz (Germany)

[**] Financial support from the Bayer Material Science AG is gratefully acknowledged.

Supporting information for this article is available on the WWW under <http://dx.doi.org/10.1002/anie.200903636>.

Table 1: Specific surface areas of chosen polymer/tungsten oxide hybrid materials and their oxidation product WO₃.^[a]

Aryl methanol derivative	hybrid material	S_g [m ² g ⁻¹] WO ₃ (400 °C) ^[b]	WO ₃ (900 °C) ^[c]
thiophene-2-methanol	7.2	39	1
furfuryl acetate	6.5	56	3
<i>p</i> -MBA	17.8	38	8
<i>o</i> -MBA	3.7	56	7

[a] Hybrid materials and oxides synthesized from 1/6 mol WCl₆ and 1 mol aryl methanol derivative. [b] Oxidized at 400 °C. [c] Oxidized at 900 °C.

The different reactivities of the aryl groups of the aryl methanol derivatives also affects the composition of the hybrid materials, which can be explained by the different nucleophilicity of the aromatic parts of the different alcohols.^[14] The polymers produced from WCl₆ and thiophene-2-methanol show signals in the ¹³C{¹H} CP MAS NMR spectrum that indicate a small amount of cross-links in the solid state (see the Supporting Information). The HMs produced from WCl₆ and furfuryl acetate are, similar to the well-known systems of furfuryl alcohol,^[3a] highly cross-linked (Figure 1).

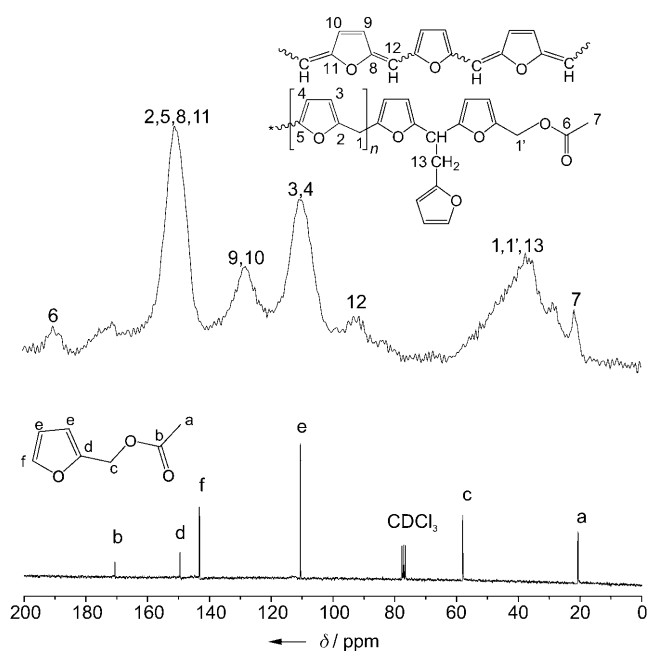


Figure 1. Top: ¹³C{¹H} CP MAS NMR spectrum of the solid composite synthesized from furfuryl acetate and WCl₆. Bottom: ¹³C NMR spectrum of furfuryl acetate in solution.

The products of the cationic Friedel–Crafts polymerization of *p*-MBA do not show any signs of cross-linking (Figure 2), but poly(*p*-methoxybenzyl alcohol) (PMBA) is still insoluble in organic solvents. One explanation for the insolubility is the existence of active cationic σ complexes after the Friedel–Crafts-polymerization. This theory is sup-

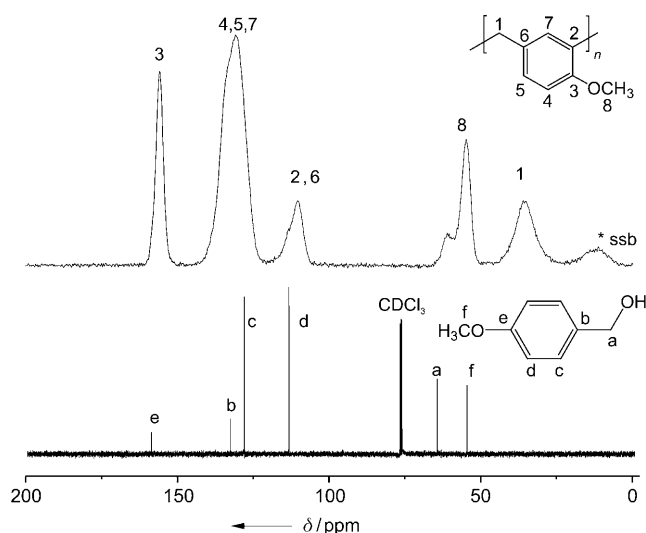


Figure 2. Top: ¹³C{¹H} CP MAS NMR spectrum of the solid composite synthesized from *p*-MBA and WCl₆. Bottom: ¹³C NMR spectrum of *p*-MBA in solution. ssb = spinning side band.

ported by the fact that the hybrid material is blue-purple colored, which is characteristic for such species.^[14] The organic PMBA component can be partly isolated by treating the HM with water and extracting with THF. The carbon content decreases from 22 % to 12–13 %, and crystalline tungsten trioxide hydrate is formed during the procedure (see the Supporting Information).

To check whether WCl₆ acts as initiator, as in a conventional cationic polymerization, or as a preferred reaction partner for the aryl methanol derivative, the influence of the aryl methanol/WCl₆ ratio on the resulting carbon content of the HMs was investigated. If WCl₆ were to act as initiator, we would expect an increase in the amount of organic monomer to lead to an increase in the molecular weight and the amount of polymer. However, an organic/inorganic HM is formed, independent of the monomer/WCl₆ ratio. In the reaction of WCl₆ with various amounts of aryl methanol, the carbon content in the case of *p*-MBA is near (22 ± 1.7) % (Figure 3). It is therefore likely that the HM is formed from an in situ monomer or from a mixture of monomers. The yields of the

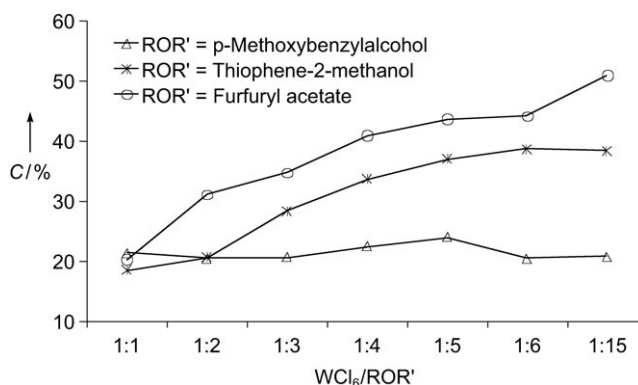


Figure 3. The polymer content (represented by the carbon content in %) of the hybrid material as a function of the WCl₆/ROR' mass ratio.

HMs for different $\text{WCl}_6/p\text{-MBA}$ ratio are approximately equal (see the Supporting Information), thus indicating the formation of similar intermediates.

The carbon contents and yields of HMs produced with thiophene-2-methanol rise steadily up to a $\text{WCl}_6/\text{alcohol}$ ratio of 1:5 and then remain constant for larger amounts of alcohol. The reactivity of the aryl group of thiophene-2-methanol is higher than that of *p*-MBA. Concentration-dependent cross-linking of the organic polymer results, which reaches its maximum at a starting-material ratio of 1:5. Above that level, excess alcohol no longer contributes to the cross-linking and can be separated. Furfuryl acetate has the highest aromatic reactivity of the investigated compounds. It was preferred to furfuryl alcohol because the acetyl chloride is released upon reaction of furfuryl acetate with WCl_6 . The extremely reactive furfuryl alcohol tends to form highly cross-linked structures, so inhomogeneous HMs result under the same reaction conditions. If furfuryl acetate, the most reactive organic component employed herein, is used, the carbon content and the yield of the resulting material both steadily increase with the proportion of furfuryl acetate. The $^{13}\text{C}\{^1\text{H}\}$ CP MAS NMR spectra indicate that the degree of cross-linking of the polymers is correlated to the nucleophilicity of the aromatic parts of the alcohols.^[15]

The tungsten trioxide was obtained from the HMs by thermal oxidation at different temperatures in air. Nanoscale tungsten trioxide is even accessible from oxidation at 400 °C. The products still contain small amounts of carbon (less than 0.5%), but they are free from chlorine. It is likely that the minimal amount of residual carbon is responsible for the stabilization of WO_3 nanoparticles. If the oxidation takes place at 900 °C, larger tungsten trioxide particles are obtained. The SEM images of the oxides obtained from HMs formed from WCl_6 and *p*-MBA are exemplary for all synthesized oxides (Figure 4). The composites synthesized from WCl_6 and furfuryl acetate or *o*-MBA were also calcined and led to WO_3 with similar nanostructures (Figure 5).

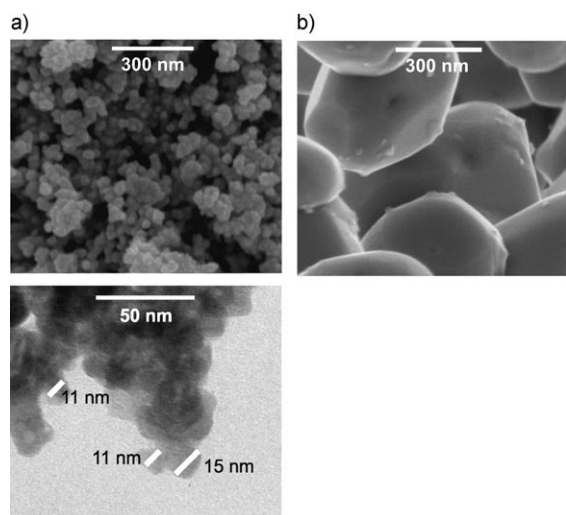


Figure 4. Electron microscope images of WO_3 synthesized by calcination of the hybrid material that was synthesized from WCl_6 and 6 *p*-MBA and calcined at a) 400 °C and b) 900 °C.

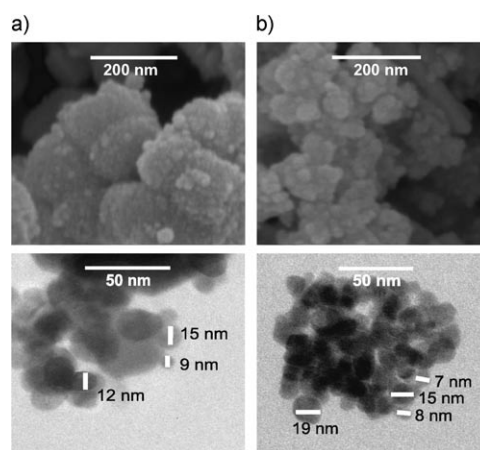


Figure 5. Electron microscope images of nanostructured WO_3 synthesized by calcination of the materials from WCl_6 and a) 6 furfuryl acetate and b) 6 *o*-MBA at 400 °C.

The XRPD patterns clearly show that the oxide materials only contain pure tungsten trioxide (see JCPDS, 01-071-0131). The diffractograms of the oxides resulting from the reaction of WCl_6 and *p*-MBA serve as a representative example for all the synthesized oxides (Figure 6). These results support the assumptions that were made on the basis of the BET surface areas (Table 1) and the electron microscopic images.

The BET surface area decreases with increasing oxidation temperature (Table 1), as expected. The largest BET surface area for tungsten oxides synthesized at 400 °C is $56 \text{ m}^2 \text{ g}^{-1}$. This result confirms that the in situ polymerization of reactive tungsten aryl methoxide adducts is a possibility for synthesizing nanoscale tungsten oxides with unprecedented BET surface areas.

In summary, it can be noted that the concept of the TP of complex monomers is not always transferable to metals with a high oxidation number or with a high Lewis acidity, because complex monomers and mixture of monomers can polymerize spontaneously. However, nanostructured hybrid materials can be produced from easily accessible educts, as shown by

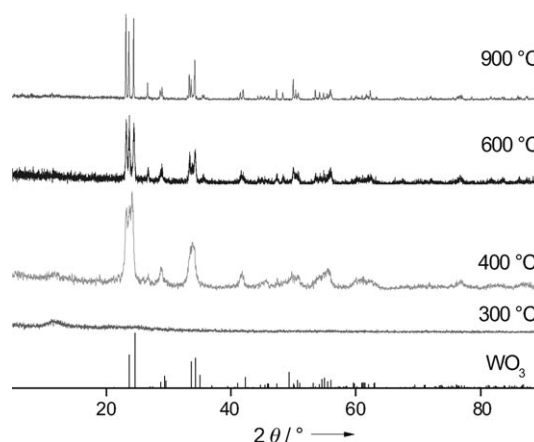


Figure 6. XRPD patterns of the oxides of the hybrid materials from WCl_6 and 6 *p*-MBA compared with WO_3 (JCPDS: 01-071-0131).

the example of WO_3 prepared by in situ TP (ISTP). WCl_6 served as a starting material for halide-free WO_3 . In contrast to large-scale production, two steps are needed to synthesize tungsten trioxide. At room temperature a hybrid material is obtained. The HM is oxidized in air and leads to tungsten oxide. Thus, the ISTP procedure offers a new perspective to synthesize industrially relevant nanomaterials. The somewhat larger synthetic effort is justified by the nanostructuring and the achievable large BET surfaces.

The ISTP procedure differs from NASG, as a WO_3 /polymer hybrid material results, as from known from TP. From this hybrid the oxide is obtained by removal of the organic polymer. In this oxidation process it is possible to adjust the particle size (see Figure 4, Figure 5, and the Supporting Information).

It is obvious that the reactive intermediate that leads to the oxidic component of the hybrid material is similar to the intermediates of the NASG. The ISTP is therefore conceptually between NASG and TP, and it builds a bridge between the two procedures (Table 2). The extension of this concept, even in combination with TP or NASG, to other metal oxides and hybrid materials, is currently being investigated.

Table 2: Comparison of the reaction steps of twin polymerization, in situ twin polymerization, and the non-aqueous sol-gel process to synthesize nanoscale metal oxides.

Experiment/result	TP	ISTP	NASG
defined monomer as starting material	yes	no	no
polymerization of the organic component	yes	yes	no
product: polymer/ MO_x hybrid material	yes	yes	no
nanoscale MO_x after isolation	yes	yes	yes

Experimental Section

In a typical hybrid material synthesis, WCl_6 (2.0 g, 5 mmol) was dissolved in anhydrous CH_2Cl_2 (400 mL) at room temperature (25°C). An aryl methanol derivative or furfuryl acetate (30 mmol) was dissolved in CH_2Cl_2 (10 mL) and added to the solution of WCl_6 . While being stirred, the solution evolved HCl, the color changed after a few seconds from red to blue, and a blue solid preprecipitated (in the case of *p*-MBA). The mixture was stirred for approximately 15 h at room temperature. Then the solid was filtered off, washed with CH_2Cl_2 , and dried under vacuum. The yield is between 31% (*p*-methoxybenzyl alcohol, *o*-methoxybenzyl alcohol) and 93% (thiophene-2-methanol, furfuryl acetate).

To obtain WO_3 , the hybrid materials were heated to 400°C or 900°C (2 K min⁻¹) in an air stream of 400 L min⁻¹ and kept there for 3 h.

Details of analytic methods are given in the Supporting Information.

Received: July 3, 2009

Published online: October 20, 2009

Keywords: nanocomposites · nanomaterials · tungsten trioxide · twin polymerization

- [1] a) G. Frenzer, W. F. Maier, *Annu. Rev. Mater. Res.* **2006**, *36*, 281–331; b) G. R. Patzke, F. Krumeich, R. Nesper, *Angew. Chem.* **2002**, *114*, 2554–2571; *Angew. Chem. Int. Ed.* **2002**, *41*, 2446–2461; c) Y. Mao, T.-J. Parka, S. S. Wong, *Chem. Commun.* **2005**, 5721–5735; d) M. E. Franke, T. J. Koplin, U. Simon, *Small* **2006**, *2*, 36–50; e) J. Park, J. Joo, S. G. Kwon, Y. Jang, T. Hyeon, *Angew. Chem.* **2007**, *119*, 4714–4745; *Angew. Chem. Int. Ed.* **2007**, *46*, 4630–4660; f) B. K. Tay, Z. W. Zhao, D. H. C. Chua, *Mater. Sci. Eng. R* **2006**, *52*, 1–48; g) J. Polleux, N. Pinna, M. Antonietti, M. Niederberger, *J. Am. Chem. Soc.* **2005**, *127*, 15595–16601.
- [2] a) N. Pinna, *J. Mater. Chem.* **2007**, *17*, 2769–2774; b) Y.-W. Jun, J.-S. Choi, J. Cheon, *Angew. Chem.* **2006**, *118*, 3492–3517; *Angew. Chem. Int. Ed.* **2006**, *45*, 3414–3439; c) N. Pinna, M. Niederberger, *Angew. Chem.* **2008**, *120*, 5372–5385; *Angew. Chem. Int. Ed.* **2008**, *47*, 5292–5304; d) M. Niederberger, G. Garnweitner, *Chem. Eur. J.* **2006**, *12*, 7282–7302; e) I. Djerdj, D. Arcon, Z. Jaglicic, M. Niederberger, *J. Solid State Chem.* **2008**, *181*, 1571–1581.
- [3] a) S. Grund, P. Kempe, G. Baumann, A. Seifert, S. Spange, *Angew. Chem.* **2007**, *119*, 636–640; *Angew. Chem. Int. Ed.* **2007**, *46*, 628–632; b) A. Mehner, T. Rüffer, H. Lang, A. Pohlers, W. Hoyer, S. Spange, *Adv. Mater.* **2008**, *20*, 4113–4116; c) S. Spange, S. Grund, *Adv. Mater.* **2009**, *21*, 2111–2116; d) S. Spange, P. Kempe, A. Seifert, A. A. Auer, P. Ecorchard, H. Lang, M. Falke, M. Hietschold, A. Pohlers, W. Hoyer, G. Cox, E. Kockrick, S. Kaskel, *Angew. Chem.* **2009**, *121*, 8403–8408; *Angew. Chem. Int. Ed.* **2009**, *48*, 8254–8258.
- [4] J. Polleux, A. Gurlo, N. Barsan, U. Weimar, M. Antonietti, M. Niederberger, *Angew. Chem.* **2006**, *118*, 267–271; *Angew. Chem. Int. Ed.* **2006**, *45*, 261–265.
- [5] A. F. Holleman, *Lehrbuch der Anorganischen Chemie*, De Gruyter, Stuttgart, **1985**, p. 1103.
- [6] E. Lassner, *Tungsten*, Kluwer Academic, New York, **1999**.
- [7] a) H. Liu, T. Peng, D. Ke, Z. Peng, C. Yan, *Mater. Chem. Phys.* **2007**, *104*, 377–383; b) A. A. Ashkarran, A. Irajadi, M. M. Ahadian, S. A. Mahdavi Ardakani, *Nanotechnology* **2008**, *19*, 195709–195718; c) G. R. Bamwenda, H. Arakawa, *Appl. Catal. A* **2001**, *210*, 181–191; d) V. Puddu, R. Mokaya, G. L. Puma, *Chem. Commun.* **2007**, 4749–4751; e) X. Z. Li, F. B. Li, C. L. Yang, W. K. Ge, *J. Photochem. Photobiol. A* **2001**, *141*, 209–217. For nonporous tungsten trioxide platelets with an average size of 200 nm × 200 nm × 10 nm, an extremely high specific surface area of about 180 m² g⁻¹ was measured: D. Chen, L. Gao, A. Yasumori, K. Kuroda, Y. Sugahara, *Small* **2008**, *4*, 1813–1822.
- [8] P. M. S. Monk, R. J. Mortimer, D. R. Rosseinsky, *Electrochromism*, VCH, Weinheim, **1995**, p. 67.
- [9] F. G. K. Baucke, B. Metz, J. Zauner, *Phys. Unserer Zeit* **1987**, *18*, 21–30.
- [10] C. G. Granqvist, *Electrochim. Acta* **1999**, *44*, 3005–3015.
- [11] a) S. H. Wang, T.-C. Chou, C.-C. Liu, *Sens. Actuators B* **2003**, *94*, 343–351; b) S. Ashraf, R. Binions, C. S. Blackman, I. P. Parkin, *Polyhedron* **2007**, *26*, 1493–1498.
- [12] S. Supothina, P. Seeharaj, S. Yoriya, M. Sriyudthsak, *Ceram. Int.* **2007**, *33*, 931–936.
- [13] R. W. Alder, P. S. Bowman, W. R. S. Steele, D. R. Winterman, *Chem. Commun.* **1968**, 723.
- [14] S. Bywater in *Cationic Polymerization*, 1st ed., (Ed.: P. H. Plesch), The Macmillan Company, New York, **1963**, pp. 307–344.
- [15] H. Mayr, T. Bug, M. F. Gotta, N. Hering, B. Irrgang, B. Janker, B. Kempf, R. Loos, A. R. Ofial, G. Remennikov, H. Schimmel, *J. Am. Chem. Soc.* **2001**, *123*, 9500–9512.